Global Change Biology

Global Change Biology (2011) **17**, 515–527, doi: 10.1111/j.1365-2486.2010.02250.x

Interpreting diel hysteresis between soil respiration and temperature

CLAIRE L. PHILLIPS*†, NICK NICKERSON‡§, DAVID RISK§ and BARBARA J. BOND†

*Terrestrial Ecosystems Research Associates, 200 SW 35th St., Corvallis, OR 97333, USA, †Department of Forest Ecosystems and Society, Oregon State University, Corvallis, OR 97331, USA, ‡Department of Earth Sciences, Dalhousie University, Halifax, NS, Canada, §Department of Earth Sciences, St Francis Xavier University, PO Box 5000, Antigonish, NS, Canada B2G 2W5

Abstract

Increasing use of automated soil respiration chambers in recent years has demonstrated complex diel relationships between soil respiration and temperature that are not apparent from less frequent measurements. Soil surface flux is often lagged from soil temperature by several hours, which results in semielliptical hysteresis loops when surface flux is plotted as a function of soil temperature. Both biological and physical explanations have been suggested for hysteresis patterns, and there is currently no consensus on their causes or how such data should be analyzed to interpret the sensitivity of respiration to temperature. We used a one-dimensional soil CO_2 and heat transport model based on physical first principles to demonstrate a theoretical basis for lags between surface flux and soil temperatures. Using numerical simulations, we demonstrated that diel phase lags between surface flux and soil temperature can result from heat and CO_2 transport processes alone. While factors other than temperature that vary on a diel basis, such as carbon substrate supply and atmospheric CO_2 concentration, can additionally alter lag times and hysteresis patterns to varying degrees, physical transport processes alone are sufficient to create hysteresis. Therefore, the existence of hysteresis does not necessarily indicate soil respiration is influenced by photosynthetic carbon supply. We also demonstrated how lags can cause errors in Q_{10} values calculated from regressions of surface flux and soil temperature measured at a single depth. Furthermore, synchronizing surface flux and soil temperature to account for transport-related lags generally does not improve Q_{10} estimation. In order to calculate the sensitivity of soil respiration to temperature, we suggest using approaches that account for the gradients in temperature and production existing within the soil. We conclude that consideration of heat and CO_2 transport processes is a requirement to correctly interpret diel soil respiration patterns.

Keywords: Fick's Law, hysteresis, Q_{10}, soil respiration, temperature

Received 27 January 2010; revised version received 6 April 2010 and accepted 15 April 2010

Introduction

Soil respiration, which is often the largest flux of CO_2 leaving terrestrial ecosystems (Ryan & Law, 2005; Jassal *et al*., 2007; Gaumont-Guay *et al*., 2008), is likely to be an important determinant of ecosystem carbon balance under future climate scenarios. The temperature sensitivity of soil respiration is one of the more basic characteristics that ecologists would like to quantify in order to predict fluxes in changing environments. However, regressions between soil respiration and temperature often have relationships that do not agree with theoretical models, such as the commonly used Arrhenius or van't Hoff type expressions (see Davidson *et al*., 2006a for a detailed discussion). Models based on simple reaction kinetics do not capture the biological and physical complexities of soil systems, including heat and gas transport dynamics (Risk *et al*., 2002; Pumpanen *et al*., 2003; Davidson *et al*., 2006b; Pavelka *et al*., 2007). While there is much agreement that more sophisticated, mechanistic models are required to describe and predict soil respiration, many suggestions have focused on improving descriptions of biological production (Trumbore, 2006; Carbone & Vargas, 2008), and the complexities of soil physical processes have not received the same level of attention.

In recent years, automated soil respiration chambers have gained widespread use, providing temporally dense datasets that reveal complex relationships between soil respiration and temperature that are not apparent with less frequent survey measurements. Many researchers who analyze data from automated chambers have observed diel hysteresis, evidenced by semielliptical shapes in regression plots of soil temperature and soil respiration (see examples in Riveros-Iregui *et al*., 2007; Bahn *et al*., 2008; Carbone & Vargas, 2008). These ellipses result from phase lags between the diel

Correspondence: C. L. Phillips, tel. +1 541 231 9823, e-mail: claire.phillips@teraglobalchange.org

signals of soil temperature and soil respiration, but there is no consensus on what causes phase lags, or how best to analyze lagged data in order to determine the temperature sensitivity of soil respiration (Pavelka *et al*., 2007; Graf *et al*., 2008; Gaumont-Guay *et al*., 2008).

Two main lines of reasoning have been proposed to explain the origins of phase lags. The first is the covariate argument, that environmental factors which oscillate out of phase with soil temperature, such as carbon supply from recent photosynthate, modify CO_2 emissions (Tang *et al*., 2005; Stoy *et al*., 2007; Vargas & Allen, 2008; Kuzyakov & Gavrichkova, 2010). The second is the heat transport argument, that soil temperature measured at an arbitrary depth is out of sync with surface efflux, due to shifts in the phase and amplitude of soil temperature with depth (Pavelka *et al*., 2007; Graf *et al*., 2008). This argument is based on the fact that soil CO_2 production in an integrated response a to nonuniform temperature profile, so temperatures measured at discrete soil depths are likely to differ in both magnitude and phase from the average temperature forcing soil CO_2 production. The covariate and heat-transport explanations are not mutually exclusive, and both factors are likely to play important roles in diel soil respiration dynamics. An additional factor that has not been discussed extensively is that gas diffusion through soil imposes a lag between the time of CO_2 production at depth and release from the soil surface.

An excellent example of how these potential explanations can act simultaneously is the multiple influences that soil moisture can have on diel soil respiration patterns. Lags between soil respiration and temperature, and the semielliptical forms produced when these variables are plotted against each other, have been shown to vary seasonally with soil moisture (Tang *et al*., 2005; Riveros-Iregui *et al*., 2007; Carbone *et al*., 2008; Vargas & Allen, 2008). All of the processes mentioned above – substrate supply, heat transport, and CO_2 diffusion – are influenced by soil moisture and can provide partial explanations for seasonal changes in diel hysteresis. Additionally, hysteresis patterns can also change day-to-day under conditions where soil moisture is fairly constant, and so diel influences from factors not wholly related to moisture should also be considered, such as photosynthetic carbon supply (Liu *et al*., 2006; Bahn *et al*., 2009), and disturbances such as atmospheric turbulence (Flechard *et al*., 2007).

Having multiple drivers which vary on a diel basis complicates the goal of measuring the temperature sensitivity of respiration *in situ*. Determining the temperature response of surface flux requires first disentangling the effects of temperature from other diel environmental drivers, and second, relating surface flux rates to nonuniform CO_2 production and temperature profiles. In this study, we aimed to provide a conceptual framework and a modeling tool for addressing both parts of this process.

To evaluate the influences of temperature on surface flux in the absence of any other controlling factors, we first determined the theoretical diel relationship between soil temperature and surface flux resulting from purely physical transport processes. Using basic principles of gas diffusion and heat transport, we simulated the expected lag times and hysteresis patterns between soil temperature and surface flux. We then performed a series of sensitivity analyses to determine the impacts on lag times of variations in soil physical factors, such as thermal diffusivity and gas diffusivity, and environmental factors, such as air temperature variation. To show the challenges and possibilities for distinguishing temperature from other diel signals, we continued by simulating increasingly complex field scenarios, modeling simultaneous changes in temperature and other environmental variables, including atmospheric CO_2 and carbon substrate supply. These simulations demonstrate how both physical and biological drivers might influence hysteresis patterns under field conditions.

To understand how transport processes impact calculations of the temperature sensitivity of soil respiration, we also used simulations to examine the accuracy of Q_{10} values calculated from regressions of surface flux and soil temperature. We identify several short-comings at diel timescales with this commonly used regression approach, and suggest potential alternatives.

Methods

Model description

We modified the one-dimensional soil CO_2 transport model described by Nickerson & Risk (2009) so that it had the following functionality: (1) a CO_2 transport component governed by Fick's First law of diffusion, (2) a heat transport component that shifts and dampens oscillating air temperatures with increasing soil depth, and (3) a simple CO_2 production function that adjusts production rate in each soil layer by the depth and temperature of the layer.

The modeled environment assumes a well-mixed atmospheric boundary layer and a soil profile of length L (m) that is divided into 100 uniform layers. Each layer has specific values for total porosity, volumetric water content, and air-filled porosity. Air-filled porosity is used in turn to calculate both gas diffusivity (D_{CO_2}) and thermal diffusivity (D_T), based on empirical relationships from the literature (details below). D_{CO_2} and D_T, along with CO_2 and temperature gradients, determine the rate of CO_2 and heat transport, respectively. For the purposes of these instructive simulations, soil physical

properties and diffusivities were assumed to be constant throughout the soil profile.

The CO_2 transport component of the model allows gas exchange between neighboring soil layers following concentration gradients. Flux rates between layers are determined with the discrete, one-dimensional form of Fick's First Law:

$$F_{ij} = -D_{ij}\frac{\Delta C_{ij}}{\Delta z_{ij}}, \quad (1)$$

where D_{ij} is the effective CO_2 diffusion coefficient between two soil layers (layer i and layer j), ΔC_{ij} is the difference in layer CO_2 concentrations ($\mu mol\,m^{-3}$), and z_{ij} is the difference in the depths (m) of the two layers. Temperature corrections for diffusivity are calculated for each layer at each model time step (1 s) as follows:

$$D_i = D_0\left(\frac{T_i}{T_0}\right)^{1.75}, \quad (2)$$

where D_0 is soil diffusivity at reference temperature T_0 (273 K) and T_i is the ambient temperature (K) of layer i.

At each model time step, a new CO_2 concentration in each layer (C_i) is calculated as function of the layer depth:

$$C_i(z,\,t) = \frac{C_i(z,t-1)\theta \times L/N + F(z-1) - F(z) + \gamma(z)}{\theta \times L/N}, \quad (3)$$

where $C_i(z,t-1)$ is the layer concentration at the previous time step, θ is the soil air-filled pore space, $F(z-1)$ is flux from the layer below (which is generally positive, representing a flux in, but the sign depends on concentration gradients), $F(z)$ is the flux from the present layer, $\gamma(z)$ is layer CO_2 production ($\mu mol\,m^{-3}\,s^{-1}$), L is the total depth of the soil column and N is the total number of soil layers.

Unless otherwise noted, biological CO_2 production decreases with soil depth according to the following exponential function (Nickerson & Risk, 2009):

$$\gamma(z, T_{ave}) = \frac{\Gamma_0}{\sum_{z=0}^{L}\exp\left(\frac{-z}{d_P}\right)}\exp\left(\frac{-z}{d_P}\right), \quad (4)$$

where T_{ave} is the average temperature of the atmosphere and profile, Γ_0 is total basal soil production at the average temperature ($\mu mol\,m^{-3}\,s^{-1}$), z is the layer depth, and d_p is the exponential folding layer, or the layer at which the proportion of total soil production remaining is $1/e$ (0.37). By manipulating d_P, CO_2 production can be confined mostly to shallow soil layers, or spread more evenly across the soil profile. A basal value for total soil CO_2 production is defined by the user and partitioned with Eqn (4) to give layer-specific basal production. At each time step, layer production is adjusted in response to the current layer soil temperature $T(z,T)$ using a modified van't Hoff relationship:

$$\gamma(z,\,T) = \gamma(z,\,T_{ave}) \times Q_{10}^{[(T(z,t)-T_{ave})/10]}. \quad (5)$$

The heat transport component of the model approximates air and soil temperature as sinusoidal curves (Hillel, 1998), where soil temperature is shifted and damped from the air temperature curve as a function of depth:

$$T(0,\,t) = T_{ave} + A_0\sin(\omega t), \quad (6)$$

$$T(z,\,t) = T_{ave} + A_0[\sin(\omega t - z/d_T)]e^{-z/d_T}, \quad (7)$$

where $T(0,t)$ is the temperature at the soil surface ($z = 0$), A_0 is the amplitude of the surface temperature fluctuation (1/2 of the total daily range), and ω is the radial frequency, which converts time to radians. For a sine wave oscillating on a period of 1 day (86 400 s), $\omega = 2\pi/86\,400$. The constant d_T is the thermal damping depth, and is defined as the depth at which temperature amplitude decreases to the fraction $1/e$. Thermal damping depth (m) is related to thermal diffusivity (D_T) as follows:

$$d_T = \sqrt{2D_T/\omega}. \quad (8)$$

One should note that the two parameters in the heat transport equations which are impacted by environment are diel air temperature amplitude (A_0), and thermal diffusivity (D_T).

Model implementation

Simulations were performed to examine (1) the impacts of model parameters on lag times and hysteresis patterns and (2) how lags affect calculation of soil respiration temperature sensitivity. We defined a set of default soil physical and environmental conditions for simulations (Table 1), based on measurements of a sandy loam soil from the HJ Andrews Experimental Forest in the western Cascades of Oregon, USA (44.2°N, 122.2°W). Further description of the site and soil is provided by Pypker *et al*. (2008). Default environmental conditions are characteristic of early summer. For sensitivity analyses, we varied each of these parameters across a large range of realistic values. Soil depth was modeled as 100 cm for all scenarios.

Realistic values for D_{CO_2} at different soil moisture contents were modeled using the relationship described by Moldrup *et al*. (2000), which expresses soil gas diffusivity as a function of air-filled porosity and soil moisture release characteristics:

$$D_P = D_0 \times (2\varepsilon_{100}^3 + 0.04\varepsilon_{100})\left(\frac{\varepsilon}{\varepsilon_{100}}\right)^{2+3/b}, \quad (9)$$

where D_P is soil gas diffusivity, D_0 is gas diffusivity in free air ($1.39 \times 10^{-5}\,m^2\,s^{-1}$ for CO_2 at 273 K and 1 atm), ε is the ambient

Table 1 Default parameters for model simulations

Parameter	Default value
Soil porosity	0.65 (v/v)
Air-filled porosity (Θ)	0.35 (v/v)
Thermal diffusivity (D_T)	$6.41 \times 10^{-7}\,m^2\,s^{-1}$
Gas diffusivity (D_{CO_2})	$1.29 \times 10^{-6}\,m^2\,s^{-1}$
Production exponential folding depth (d_P)	10 cm
Q_{10}	2
Average air and soil temperature (T_{ave})	15 °C
Air temperature amplitude (A_0)	7.5 °C
Total basal CO_2 production (Γ_0)	$1.5\,\mu mol\,m^{-2}\,s^{-1}$
Atmospheric CO_2	385 ppm

Deviations from these values are noted in text or figures.

air-filled porosity, ε_{100} is the air-filled porosity at −100 cm H_2O tension (~10 kPa), and b is the slope from a log plot relating volumetric water content to soil water potential. We used coefficients determined from 12 intact soil cores taken from the HJ Andrews Experimental Forest. Moisture-release coefficients were determined by treating cores on pressure plates at pressures ranging from 10 to 50 kPa.

To parameterize D_T at different moisture levels, we used a published dataset for a sandy-loam soil of D_T measurements from intact soil cores across air-filled porosities ranging 0–0.60 (Ochsner *et al*., 2001). To interpolate between measured porosities we fit the data with a second-order polynomial.

Simulations were initiated with a spin-up period for modeled CO_2 flux to stabilize. The spin-up period was deemed sufficiently long when daily maximum soil surface flux values were constant for at least 5 consecutive model days. To minimize spin-up time, simulations were initialized with the steady-state solution proposed by Cerling *et al*. (1991) for a uniform profile. The model was solved by Euler integration with a computation time step for all simulations of 1 s, and model output was recorded every 300 s.

Two synthetic tests were conducted to examine the performance of the CO_2 transport component under steady-state and transient conditions. The steady-state test served to assess numerical errors associated with discretizing the soil profile into layers. This test entailed modeling uniform production profiles across a range of gas diffusivities, and comparing the modeled concentration profiles to Cerling's steady-state solution. We found soil concentration errors due to discretization to be <0.5% across all diffusivity levels. The transient test examined time lag errors related to iterating the model in discrete time steps. We varied CO_2 concentration at the upper boundary layer (atmosphere) as a sinusoidal wave, and compared the phase lags between peak CO_2 concentrations in the atmosphere and soil with the theoretical phase lag described by Beltrami (1996):

$$\delta = \frac{z}{2}\sqrt{\frac{\tau}{\pi \times D_{CO_2}}}, \quad (10)$$

where δ is the phase lag (s), z is soil depth (m), τ is the period over which atmospheric CO_2 oscillates (1 day or 86 400 s), and D_{CO_2} is the effective CO_2 diffusivity of soil ($m^2\,s^{-1}$).

Comparison of apparent and actual Q_{10} values

We examined how varying model parameters affected calculation of Q_{10} values with a widely used regression approach, which relates the natural logarithm of surface flux to soil temperature at an arbitrary depth (Pavelka *et al*., 2007):

$$\ln R = \alpha T + \beta, \quad (11)$$

where R is surface flux, T is soil temperature, and α and β are coefficients estimated from linear least squares regression. The Q_{10} of surface flux was calculated as

$$Q_{10} = e^{10^*\alpha}. \quad (12)$$

We call these Q_{10} values from *post hoc* calculations 'apparent Q_{10} values' to contrast them with the input Q_{10} used to parameterize the model (generally 2.0). It should be noted that in these simulations a small amount of diel variation in surface flux resulted from the temperature sensitivity of CO_2 diffusivity [Eqn (2)], rather than from the temperature sensitivity of CO_2 production. The variation in surface flux resulting from the temperature sensitivity of D_{CO_2} was negligible, however, accounting for $< \pm 1\%$ change in respiration when temperature was varied $\pm 15\,^{\circ}C$ over a 24 h period (see the supporting information for more details).

Results

Impacts of transport-related lags on regressions of surface flux and soil temperature

Owing to the attenuation and phase shift of soil temperatures with increasing depth, the relationship between modeled surface flux and soil temperature varied with soil temperature measurement depth (Fig. 1). Plots of surface flux against soil temperature produced hysteresis loops which changed in three respects with increasing depth: their rotational direction (see arrows in Fig. 1), their roundness or narrowness (minor radius), and the orientation of their principal axes. All three of

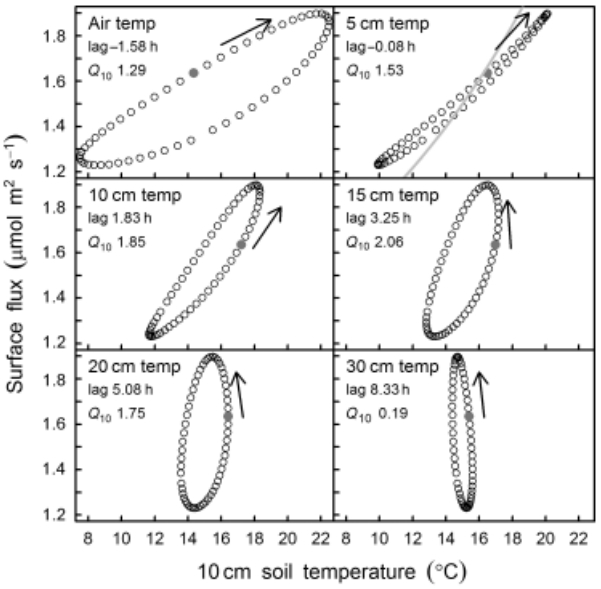

Fig. 1 Diel hysteresis between surface flux and soil temperature at several depths, and apparent Q_{10} values calculated from least squares regression (see text for details). Solid points show time = 12 h and arrows indicate the direction of hysteresis over time. Gray line represents the fitted mean that would produce an apparent Q_{10} equal to the input value of 2. $D_T = 5 \times 10^{-7}\,m^2\,s^{-1}$ (same data as bottom panel of Fig. 3). Negative lags indicate surface flux reaching a maximum before temperature whereas positive lags indicate temperature peaking first.

these qualities were functions of the lag time between surface flux and soil temperature. At depths where soil temperature reached a daily maximum before surface flux (e.g. at soil depths above 5 cm in Fig. 1), hysteresis loops rotated clockwise, while at deeper depths where soil temperatures peaked after surface efflux, the loops rotated counter clockwise.

The narrowness, or minor radius, of hysteresis loops, as well as the orientation, can be described as functions of lag time using principles of harmonic motions. As adapted from Beltrami (1996), two sine waves that are offset by a lag give the equation of an ellipse when superimposed perpendicularly:

$$R = R_A \frac{T}{T_A} \cos\delta + R_A \sqrt{\left(1 - \frac{T^2}{T_A}\right)} \sin\delta, \qquad (13)$$

where R_A and T_A are the amplitudes of respiration rate and temperature, respectively, R and T are instantaneous respiration rate and temperature, respectively, and δ is the lag, or the difference in phase between the temperature and respiration waves (expressed in radians). When the lag is a full period (equivalent to 0 or 24 h), the expression of an ellipse simplifies to a straight line with positive slope. For a 1/2 period (12 h), the expression simplifies to a straight line with negative slope. For lags of 1/4 period (6 h), the result will be a horizontal ellipse. Our results show it is possible to observe any of these orientations within a soil profile. Lags up to and exceeding 24 h occurred for deep reference soil temperatures, particularly at low thermal diffusivities, which slow propagation of temperature through the soil. With a reference soil temperature at 30 cm depth, lags exceeded a full 24 h period when values of D_T became $<2 \times 10^{-7}\,m^2\,s^{-1}$.

Even at soil depths where there was no time lag between temperature and surface flux, regressions did not produce close estimates of respiration temperature sensitivity. For the example in Fig. 1, surface flux was nearly synchronized with 5 cm soil temperature and little hysteresis was apparent. However, the least squares estimate of Q_{10} was 1.53, which is substantially smaller than the actual Q_{10} of 2.0 used to parameterize the model, shown in gray. The closest approximation of the input Q_{10} occurred at 15 cm depth, despite pronounced hysteresis at this depth. This depth also is not associated with an area where most production occurs. The production profile for this simulation declined exponentially with depth, with more than two-thirds of CO_2 production occurring above 10 cm ($d_p = 10$ cm). There was no discrete soil depth where temperature was synchronized with surface flux and approximated the correct Q_{10} value.

We found that in general, the strength of correlation (R^2) between surface flux and soil temperature measured at an arbitrary depth was strongly influenced by transport-related lags (Fig. 2a), and R^2 was a poor statistic for predicting what soil depth would return an accurate Q_{10} (Fig. 2b). To examine the influence of lag time on R^2 and Q_{10} values estimated from regressions of surface flux and soil temperature, we varied thermal diffusivity in the model, which as described below was the model parameter with the largest impact on lag time (Fig. 4a). We then examined regressions between surface flux and soil temperature using reference depths of 5, 10, 15, and 20 cm. We found R^2 had a predictable and regular relationship with lag time, regardless of the reference temperature depth (Fig.

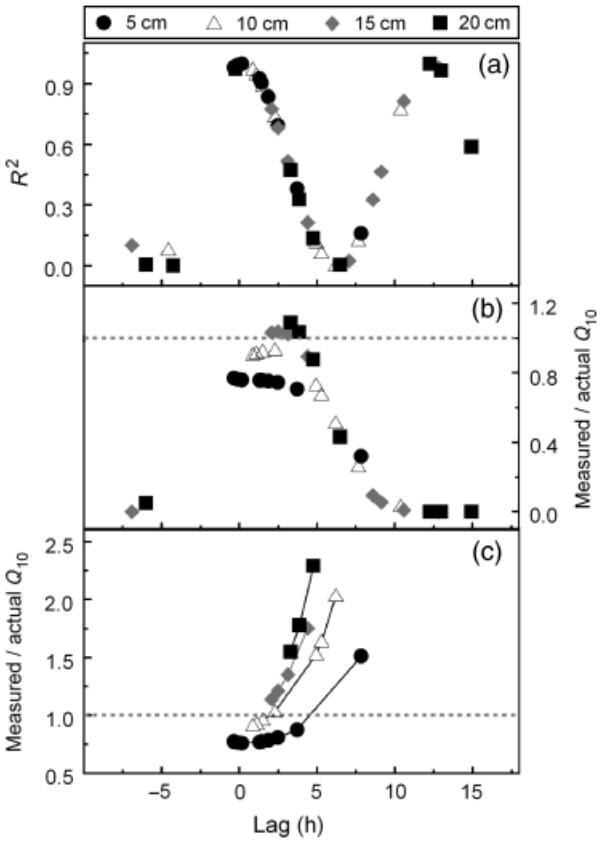

Fig. 2 Impact of phase lags on R^2 and apparent Q_{10} calculated from regressions of surface flux and soil temperature. (a) R^2 for regressions with soil temperature at reference depths of 5 cm (●), 10 cm (△), 15 cm (◆), and 20 cm (■). Lag time was varied by changing thermal diffusivity from 1×10^{-8} to $9 \times 10^{-7}\,m^2\,s^{-1}$, as in Fig. 4a. (b) Apparent Q_{10} as a function of phase lag, normalized by the actual Q_{10} used to parameterize the model. (c) Same as (b), but surface flux data was shifted to be in-phase with soil temperature before calculating apparent Q_{10}. Apparent Q_{10} approached infinity with increasing phase lag, so only normalized values <2.5 are shown for clarity.

2a). R^2 peaked at 0 and 12 h lag, which is the when the expression for an ellipse simplifies to a straight line, and reached a minimum at 6 and 18 h lag, which is when the expression produces a horizontal ellipse. As described above [Eqn (13)], the narrowness, or minor radius of hysteresis loops can be described as a function of lag time, and as hysteresis loops become more round the strength of correlation decreases, and as they become more narrow the strength of correlation increases.

The apparent Q_{10} values calculated from regressions were also related to lag time, but the form of the relationship was different from the form of the R^2 relationship (Fig. 2b). As a result, the conditions providing the highest R^2 values did not produce the most accurate Q_{10} values. The most accurate Q_{10} estimates coincided with conditions which produced lag times of 3–4 h, and corresponded with a wide range of R^2 values. The Q_{10} and lag relationship differed slightly for each reference depth because the slope of least squares regression, and therefore the Q_{10}, is also influenced by the amplitude of soil temperature variation at the reference soil depth [Eqn (13)].

Attempting to remove the lag by shifting surface flux data to be in-phase with soil temperature data before calculating the regression did not systematically improve estimates of Q_{10} values (Fig. 2c). Calculated Q_{10} values increased exponentially with the magnitude of the phase adjustment. For adjustments exceeding a few hours, this approach produced Q_{10} values many times greater than the Q_{10} used to parameterize the model. This indicates that knowing the lag time that is due to heat and gas transport does not readily help to determine meaningful Q_{10} values. Even after adjusting for transport-related lags, the problem remains that no single reference soil depth consistently approximates the average temperature across the whole soil production profile.

These examples demonstrate that it is best to consider temperatures across the production profile to understand temperature–respiration relationships; however, for practical purposes, temperature measurements in field studies are often restricted to one or a few discrete soil depths. In order to strengthen conceptual links between processes that take place across the entire soil production profile, and patterns that may be observed in field data, for the remainder of this article we show most results using an arbitrary soil temperature depth of 10 cm. Also, because our simulations use an exponential relationship between temperature and CO_2 production, the time offsets between daily maximum respiration and temperature differ slightly from the time offsets between minimum values. For simplicity, we only report lag times between maxima, and note when trends differ for lag times between minima.

Sensitivity of lag time to thermal diffusivity

Thermal diffusivity (D_T) influenced the speed with which changes in air temperature propagated through soil, and the depth to which diel variations in air temperature were detectable (Fig. 3). As D_T was increased in the model, changes in air temperature propagated through soil more quickly, which shortened lags between soil temperatures and surface flux. Variations in D_T had a larger effect on lag times than any other single factor we examined, although the effect was nonlinear (Fig. 4a). Lag times varied sixfold for values of D_T within the range of $1–10^{-7}\,m^2\,s^{-1}$, which is the approximate range for mineral soils experiencing normal field moisture levels (Ochsner *et al*., 2001). Lag times increased substantially for lower D_T values in the range of $1–10^{-8}\,m^2\,s^{-1}$, which corresponds with the range for organic soils (Hillel, 1998).

Sensitivity to CO_2 diffusivity, production depth

In contrast to D_T, large changes in simulated D_{CO_2} had a relatively small effect on lags between surface flux and

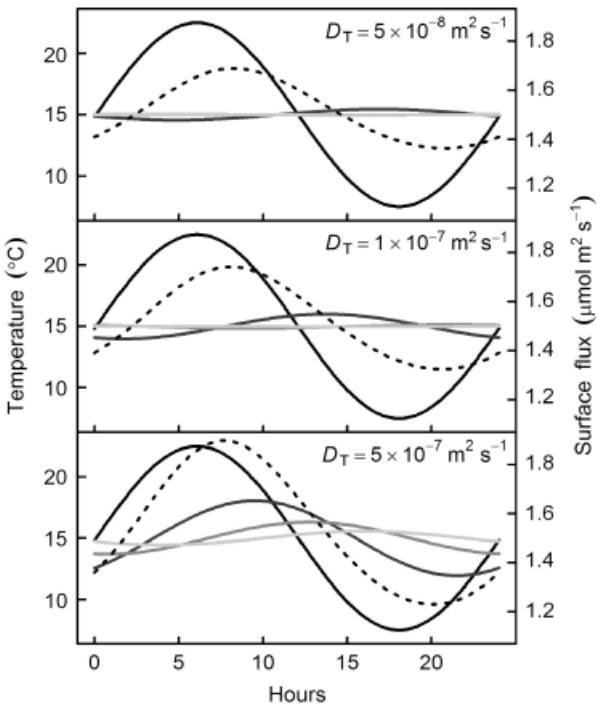

Fig. 3 Effect of thermal diffusivity, D_T, on soil temperatures at several depths (solid lines) and surface CO_2 flux (dotted line). Soil temperature depths from darkest to lightest are: soil surface, 10, 20, and 30 cm depth. See Table 1 for values of other input parameters.

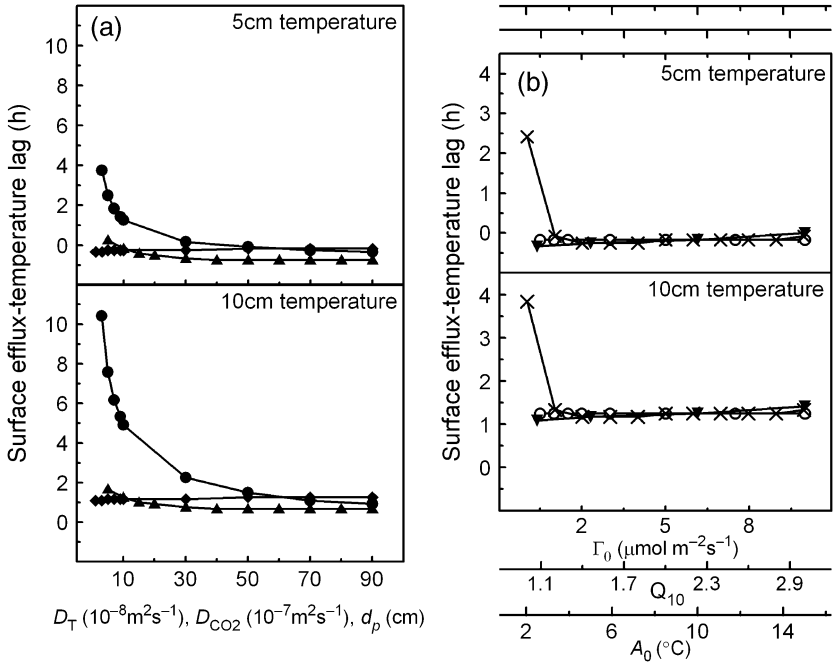

Fig. 4 Sensitivity of lag time to soil and environmental parameters. (a) Thermal diffusivity, D_T (●); CO_2 diffusivity, D_{CO_2} (◆); and exponential folding depth for CO_2 production, *dp* (▲). (b) Basal total CO_2 production, Γ_0 (○); Q10 temperature sensitivity (×); and diel air temperature amplitude, A_0 (▼).

soil temperature (Fig. 4a), but D_{CO_2} nevertheless had unique and complex impacts that are important for interpreting temperature–respiration relationships. We found that lags could occur not only between surface flux and soil temperature, but also between soil CO_2 concentrations and temperature measured at the same depth (Fig. 5a). Lags between soil CO_2 and temperature at the same depth were particularly pronounced at low D_{CO_2}. Low gas diffusivity increased the residence time of soil CO_2, causing delayed responses in CO_2 concentration to soil temperature changes. While lags between CO_2 concentration and soil temperature decreased as D_{CO_2} was increased in the model, lags between surface flux and soil temperature sometimes showed the opposite response. D_{CO_2} impacts on surface flux lags depended on both the distribution of CO_2 production, and the depth of the reference soil temperature. When production was concentrated near the surface (Fig. 5b), the phase of the surface flux sine wave shifted closer to the waves of near-surface temperatures as D_{CO_2} increased, but also shifted farther away from the waves of deep soil temperatures. At reference soil depths near the surface, lags between surface flux and soil temperature decreased with increasing D_{CO_2}, but at deeper reference depths lags increased. In contrast, when CO_2 production was uniformly distributed throughout the soil (Fig. 5c), a greater proportion of CO_2 came from deep soil layers, and increasing D_{CO_2} caused the phase of the surface flux sine wave to shift closer to deep soil temperatures and to shift farther from air and near-surface temperature.

We also explored the sensitivity of lags to variations in production depth when D_{CO_2} was held constant. Figure 4a shows changes in the depth of CO_2 production with respect to the exponential folding depth, d_P, where a higher d_P indicates production is spread more evenly across the soil profile and a lower d_P indicates production is confined more to the shallow subsurface. Changes in production within the shallow subsurface (e.g. an increase in d_P from 5–10 cm) had greater impacts on lag time than changes in production deeper within the soil (e.g. an increase in d_P from 60 to 70 cm), because most diel variability in soil temperature occurred at shallow depths. Even at very high D_T, diel temperature oscillations occurred primarily within the top few centimeters of soil. For example, for the maximum D_T plotted in Fig. 4a ($D_T = 9 \times 10^{-7}\,m^2\,s^{-1}$), temperature amplitude decreases to approximately one-third by 16 cm depth. CO_2 production deep in the soil profile varied little throughout the day because it experienced a relatively constant temperature environment, so increasing production from deep soil did little to shift diel respiration oscillations.

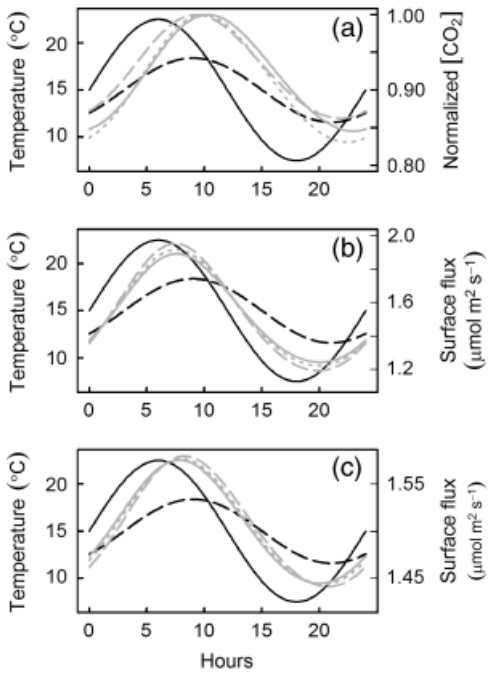

Fig. 5 Effect of CO_2 diffusivity on soil CO_2 concentrations and surface fluxes. (a) CO_2 concentration at 10 cm depth for three levels of D_{CO_2}: 5×10^{-7} (solid gray), 1×10^{-6} (dotted gray), 5×10^{-6} (dashed gray). Air temperature (solid black) and 10 cm soil temperature (dashed black) are also shown. (b) Same as (a) except gray lines represent surface CO_2 flux. (c) Same as (b) except CO_2 production was uniformly distributed across soil profile, rather than decreasing exponentially with depth.

Sensitivity to basal respiration rate and other environmental variables

Further sensitivity analysis revealed the general principle that variables which caused nonuniform changes in temperature or respiration across the soil profile tended to impact lag times. For example, changing the diel amplitude of air temperature (A_0) tended to impact lags by altering temperature variation at shallow soil depths to a greater extent than deeper soil depths. Also, changing the temperature sensitivity of CO_2 production by altering Q_{10} in the model affected lags by altering the proportional contribution from soils of different temperatures (Fig. 4b). See also the supporting information.

In contrast, increases in the basal CO_2 production rate did not influence lags. Changing basal production rate alone did not alter the proportional contribution from each soil layer to surface flux.

Effects of soil moisture on phase lags

To model the physical effects of soil moisture on lags, we allowed both D_T and D_{CO_2} to vary simultaneously as functions of air-filled porosity (Fig. 6a and b). D_T and D_{CO_2} have different relationships with soil moisture: heat propagates more quickly through water than through air-filled pore spaces, whereas CO_2 propagates more quickly through air-filled pores than through water. As simulated soil moisture was decreased, this caused an increase in D_{CO_2} and a decrease in D_T, but both had the same effect of increasing lag time between surface flux and 10 cm soil temperature (Fig. 6a), for reasons described above. As the lag time between surface flux and 10 cm soil temperature increased under dry conditions, hysteresis loops also became less linear and more elliptical in shape.

To demonstrate some of the potential impacts of moisture on biological activity, we added an additional level of complexity to the moisture simulation by decreasing basal CO_2 production rate as a linear function of soil dryness (Fig. 6c and d). While this simple linear approximation may not be realistic for very high soil moistures, it is likely to represent respiration responses to drier soil moisture conditions. As soil moisture was decreased in the model, the diel amplitude of surface flux decreased, and hysteresis appeared to become more linear and horizontal (Fig. 6d). This occurred as a result of the magnitude and daily range of respiration changing, rather than a change in the orientation of the ellipses. Lags, which control the shape and orientation of hysteresis loops, remained unaffected by altered production rates (Fig. 6c). As mentioned above, simulated changes in basal production rate alone did not affect lag times unless the distribution of production was also changed.

Diel variation in atmospheric CO_2

Concentrations of atmospheric CO_2 within and near plant canopies often vary on a diel basis, due to plant gas exchange taking up CO_2 during the day and releasing CO_2 at night (Liu *et al.*, 2006). We simulated diel oscillations in atmospheric CO_2 as a sinusoidal wave with a daily range of 50 ppm. Data from the HJ Andrews Experimental Forest indicated that daily minimum CO_2 concentration at the soil surface may be lagged from maximum temperature by as much as ± 5 h, so we hypothesized that diel changes in atmospheric CO_2 could modify surface flux and contribute to diel hysteresis between surface flux and temperature. Our simulations indicated, however, that atmospheric CO_2 has a negligible effect on flux rates, particularly when compared with effects of temperature variation. When air and soil temperature were held constant, varying atmospheric CO_2 alone changed surface flux rates by $<0.5\%$. In contrast, when diel temperatures varied even moderately, CO_2 production required little

temperature sensitivity to swamp the effects of atmospheric CO_2 variations.

Changing substrate supply

Several lines of evidence have indicated close links between canopy carbon supply and soil respiration rates, including phloem girdling studies (Högberg *et al*., 2001; Tedeschi *et al*., 2006), studies across natural gradients of root activity (Tang *et al*., 2005), lag analyses between canopy variables and soil respired $\delta^{13}CO_2$ (Fessenden & Ehleringer, 2003; McDowell *et al*., 2004; Ekblad *et al*., 2005; Kodoma *et al*., 2008), and isotopic labeling studies of photosynthate (Högberg *et al*., 2008; Bahn *et al*., 2009). We simulated potential impacts of diel variations in subsurface photosynthate supply on hysteresis in the respiration vs. temperature relationship. There is much uncertainty regarding the specifics of phloem loading to roots and how much respiration responds to fluctuations in carbon supply, and we used a simple approach of modeling diel variation in photosynthate supply as a linear function of photosynthetic active radiation (PAR), increasing basal soil CO_2 production rate from $1.5\,\mu mol\,m^{-2}\,s^{-1}$ at night to $3\,\mu mol\,m^{-2}\,s^{-1}$ in response to peak PAR over a 12 h photoperiod (Fig. 7a). As phloem transport may delay the supply of carbon substrates belowground, we also simulated a range of time offsets between peak PAR and

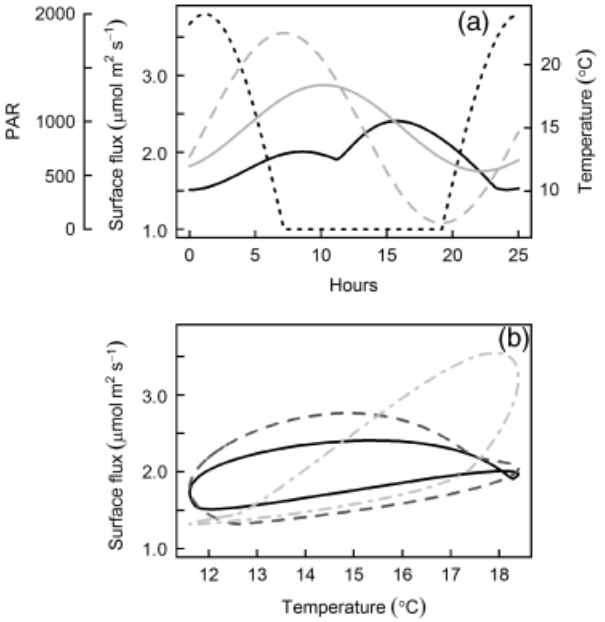

Fig. 7 Potential responses of soil respiration to diel changes in photosynthate supply. (a) Diel changes in photosynthetic active radiation (PAR) (dashed black), air temperature (dashed gray), 10 cm soil temperature (solid gray), and surface CO_2 flux (solid black). In this example, subsurface carbon supply peaked 16 h after PAR. (b) Hysteresis between surface flux and 10 cm soil temperature for various offsets between peak PAR and peak subsurface carbon supply: 16 h offset [solid black, same as in (a)], 20 h offset (dashed dark gray), and 26 h offset (dot-dashed light gray).

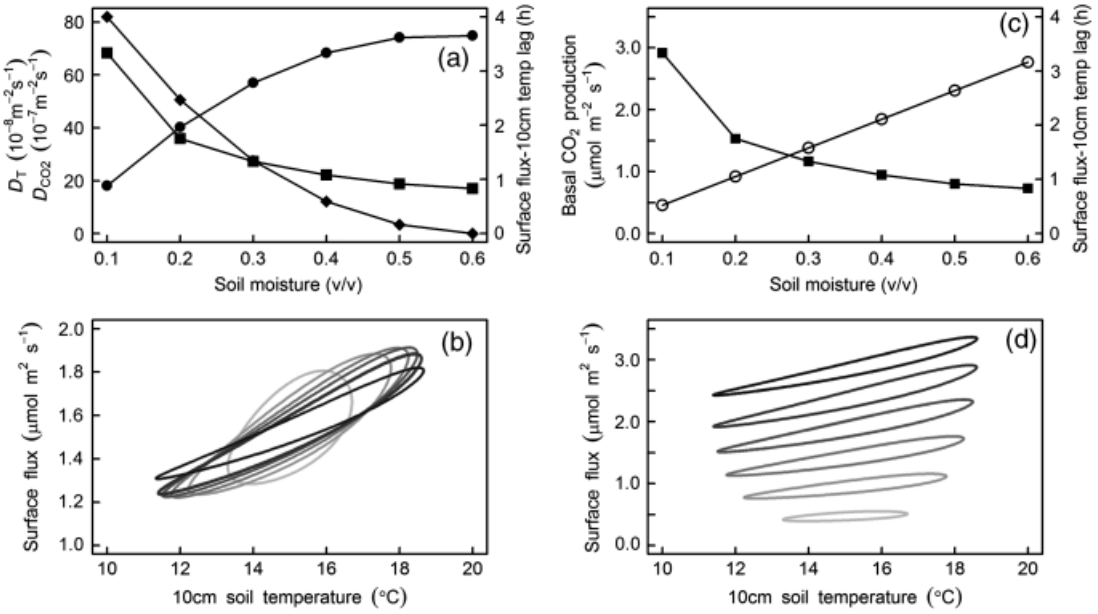

Fig. 6 (a) Effect of moisture on thermal diffusivity (●), CO_2 diffusivity (◆), and the lag time between surface flux and 10 cm soil temperature (■) for a uniform sandy-loam soil. (b) Surface flux hysteresis for moisture-dependent conditions shown in (a). From lightest to darkest: 5%, 15%, 25%, 35%, 45%, and 55% water content (v/v). (c) Changes in total basal CO_2 production (○) were added to simulations, but had no effect on lag times (■). (d) Corresponding surface flux hysteresis. From lightest to darkest: 5–55% water content (v/v), as in (b).

peak subsurface photosynthate supply (6–26 h). Some studies have suggested lags in soil respiration responses of less than a day (Tang *et al*., 2005), while others have suggested lags ranging 1–8 days (Högberg *et al*., 2001; McDowell *et al*., 2004; Mencuccini & Höltta, 2010); however, for illustrative purposes we focused on potential short-term responses to photosynthesis over the course of approximately 1 day. Because the timing and magnitude of impacts from photosynthetic carbon supply are likely to vary substantially (Kuzyakov & Gavrichkova, 2010), our goal was to emphasize only the gross patterns that could result from the combined influences from photosynthetic carbon supply and physical transport processes.

Diel variations in substrate supply substantially modified surface flux and produced hysteresis relationships with complex shapes (Fig. 7b). Although the shapes were quite variable depending on the timing of peak substrate supply, there were some consistencies among the curves that may be useful for interpreting field data. The hysteresis loops were consistently flatter on the bottom, corresponding with periods when PAR-dependent substrate supply ceased and respiration responded only to soil temperature. For large time offsets between substrate supply and soil temperature, soil respiration also exhibited double peaks over the course of the day, peaking once in response to maximum carbon supply and again in response to maximum temperature (Fig. 7a).

Discussion

The heat and CO_2 transport model described here demonstrates that purely physical drivers can have strong influences on diel dynamics of surface flux, and if transport-related lags are not accounted for, these influences may obfuscate the interpretation of the temperature sensitivity of soil respiration. Interpreting diel dynamics has two distinct but related challenges, discussed below: first, distinguishing the effects of temperature variation from other factors, and second, determining the temperature sensitivity of respiration given nonuniform soil temperature and production profiles.

Effects of soil moisture

Soil moisture can have multiple biological and physical influences on soil respiration, making it challenging to distinguish temperature and nontemperature influences on soil respiration across moisture conditions. We examined potential impacts of moisture on diel respiration dynamics both with and without biological responses to moisture. When only soil physical processes were represented in the model, decreasing soil moisture caused phase lags between surface flux and soil temperature to increase, and also caused diel hysteresis to become more pronounced (Fig. 6a and b). These purely physical trends are consistent with field observations in several studies. Under oak canopies, Tang *et al*. (2005) observed increasing lag times between surface flux and soil temperature at 8 cm depth as soils dried, although they attributed the lag to the influence of tree photosynthesis on respiration of the rhizosphere rather than to gas and temperature transport processes (discussed more below). Similarly, in mixed conifer forests (Vargas & Allen, 2008) and in shrub ecosystems (Carbone *et al*., 2008), the periods of most pronounced diel hysteresis coincided with the driest parts of the growing season.

The results from the these field studies seem to conflict with findings of Riveros-Iregui *et al*. (2007), who observed less pronounced hysteresis between soil CO_2 concentrations and temperature at 20 cm depth as soil dried. We found, however, that transport-related lags could occur not only between surface flux and soil temperature, but also in the type of measurements made by Riveros-Iregui *et al*., between CO_2 concentrations and soil temperatures measured at the same depth (Fig. 5a). Lags between soil CO_2 and temperature at the same depth consistently decreased as D_{CO_2} was increased in the model, opposite of how lags between surface flux and shallow soil temperatures behaved (Fig. 5b). In addition, we showed a potential biological explanation for decreased hysteresis with drying. When CO_2 production declined at low moistures, the magnitude and diel range of surface flux and subsurface concentrations decreased (Fig. 6c and d), which caused hysteresis to appear less pronounced and more linear at low moisture.

These examples demonstrate the difficulty of teasing apart moisture-dependent biological and physical processes that are potential drivers of diel respiration patterns. For example, it would be logical to interpret an increase in lag between surface flux and soil temperature as the soil dries as a product of substrate limitations (Carbone *et al*., 2008). Substrate limitations are indeed coupled with soil moisture, since low moisture can reduce canopy production and allocation of photosynthate belowground (Irvine *et al*., 2002, 2005), and also reduce diffusion of carbon substrates through soil (Davidson *et al*., 2006a). But increasing lags can also result from moisture influences on D_T and D_{CO_2} (Fig. 6a), so it is unlikely that changes in lag times and diel hysteresis would be due to substrate limitations alone. Similarly, declines in the amplitude and apparent tem-

perature sensitivity of surface flux with decreasing soil moisture have been attributed to reduced substrate supply, although heat transport effects produce similar results (Fig. 6b).

Detecting effects of factors other than temperature on diel surface flux patterns

Numerical simulations provide a theoretical limit to the impact of soil physical processes on lag times. We found that phase lags between surface flux and a reference temperature at 10 cm depth are between 1 and 4 h for mineral soils across a wide range of soil physical and environmental conditions (Figs 4 and 6). Lag times greater than this may be indicative of other biological factors influencing soil respiration. For example, Tang *et al*. (2005), found an approximately four hour lag between soil surface flux and temperature at 8 cm depth under an oak tree canopy, and no lag in an adjacent area of dead annual grasses. This large difference in lag times is unlikely to be a result of physical processes alone, since soil temperature data indicate D_T was similar in the two locations. As Tang *et al*. concluded, photosynthetic carbon supply may have influenced the different diel patterns in these two locations.

Asymmetrical time series or hysteresis patterns also provide a tool for detecting impacts of environmental factors other than temperature. The simulations of diel changes in substrate supply (Fig. 7) demonstrated that asymmetrical hysteresis patterns can develop in response to processes that are limited to a portion of the day only, such as photosynthesis. This example also demonstrated that double peaks can form in diel time series of surface flux when peak carbon supply is offset by a long period from peak temperature. Carbone *et al*. (2008) also observed daily double peaks in field measurements of shrub and grassland ecosystems, particularly during parts of the growing season when soil respiration was most active. Asymmetrical diel patterns such as these cannot be accounted for by temperature alone and must be attributed to influences from more than one factor.

At a minimum, by measuring both air and soil temperature, or still better, measuring soil temperature at more than one depth, one can calculate soil thermal diffusivity to obtain a rough estimate of theoretical lags between soil temperature and surface flux due to heat transport. The time difference between peak temperatures measured at several soil depths can be used to constrain D_T (Beltrami, 1996), which was shown to influence expected lag times more than any other single factor we examined. Even without more detailed information on other parameters, an estimate of D_T can provide a rough approximation of expected lag times (e.g. Fig. 4). Because soil moisture has a large influence on D_T, such estimates may be particularly helpful for researchers trying to account for changes in diel respiration–temperature relationships over a range of moisture conditions.

The heat and gas transport model used in this study can be extended to simulate field studies, and may provide an approach to tease apart influences of temperature from other factors that have diel periodicity. Detailed environmental data and soil physical parameters are required to drive the model; however, such data are becoming increasingly available. The transport equations are limited, however, to conditions where soil heat transport is dominated by conduction and CO_2 transport is dominated by diffusion. More complex transport functions would be required to simulate heat transport in flows of soil water, or to simulate mass flow of CO_2 in response to pressure gradients. The model also emphasizes physical processes, and was less rigorous for representing biological relationships. Our approach for simulating diel variation in photosynthetic carbon supply was simplistic compared to the vegetation-specific model of phloem transport by Mencuccini & Höltta (2010), but could be readily coupled to such plant physiological models.

Impacts of diel dynamics on interpretation of temperature sensitivity

A related issue to distinguishing temperature and non-temperature respiration responses is describing the temperature sensitivity of soil respiration from diel datasets. Without any change to the true temperature sensitivity of soil respiration, phase lags can alter the orientation of regressions between surface flux and soil temperature, and impact least squares fits to the data. The fact that the apparent temperature sensitivity of soil respiration differs depending on the depth where temperature is measured has been described by others (Pavelka *et al*., 2007; Graf *et al*., 2008). Less widely appreciated, perhaps, is the fact that Q_{10} estimates are related to the orientation of hysteresis loops, and can themselves be described as functions of lag times [Eqn (13) and Fig. 2].

There are several inherent problems with estimating respiration temperature sensitivity by regressing surface flux and soil temperature. The first problem is identifying an appropriate soil temperature reference depth, because R^2 relates primarily to how close the phases of surface flux and soil temperature are to one another (Fig. 2a), and does not predict the depth

which returns the most accurate Q_{10} value. Furthermore, the depth where soil temperature produces the most accurate Q_{10} can be below the portion of the soil profile where most CO_2 production occurs (Fig. 1). Neither the depth where R^2 is highest nor the depth where apparent Q_{10} is most accurate have mechanistic significance, they are coincidentally associated with phase lags that produce interesting ellipses when surface flux and soil temperature are plotted perpendicularly. Using transport models, it may be possible to predict the depth that produces the most accurate Q_{10} value. Graf *et al*. (2008) attempted this approach to determine the depth where Q_{10} should be measured, using a physical model of soil respiration similar to the one presented here. In simulations spanning several model years, they examined the sensitivity of Q_{10} uncertainty to soil physical and environmental parameters. Their simulations demonstrated two important points that are consistent with our results from diel simulations: that shallow depths underestimate Q_{10} values, and that the depth of maximum correlation between surface flux and soil temperature is different than the depth returning the input Q_{10}. These results suggest that transport effects do not only create analysis challenges in diel datasets, but at longer timescales as well.

The underlying problem with estimating temperature sensitivity from surface flux is that surface flux is an integrated response to temperature across the soil profile, not just to soil temperatures at a single depth. Reichstein *et al*. (2005) presented a potential alternative for estimating soil respiration Q_{10} values, by using a statistical model that represents surface flux as the summation of multiple fluxes from different depths, and includes soil temperature measured at each depth. Using temperatures from two depths, the authors were able to explain more than 95% of the diel variation in surface flux data, as compared with only 80% when using soil temperature from a single depth. The multiple-source model also calculated higher Q_{10} values than a single-source model. Results from our study and Graf *et al*. indicate Q_{10} values are generally underestimated with a single, shallow reference temperature, so the dual source model may estimate Q_{10} more accurately.

An alternative approach used by Risk *et al*. (2008) involved quantifying CO_2 production within the soil profile, and estimating temperature sensitivity by comparing production and temperature at the same depth. Fluxes within the soil can be determined from changes in CO_2 concentration over time. Soil profiling systems that are well-suited to this approach are becoming more widespread, and future work should further assess the potential for this approach and its limitations under non-steady-state conditions.

Even these alternative approaches are not immune, however, to influences from environmental variables other than temperature. Given that factors other than temperature are likely to influence diel patterns of soil respiration under field conditions, we recommend caution in interpreting any apparent relationship between soil respiration and temperature at diel timescales as a true measure of temperature sensitivity.

In conclusion, high-frequency soil respiration measurements have important potential for identifying influences from multiple environmental factors. However, heat and gas transport creates lags between surface flux and soil temperature that can easily be misinterpreted and obscure the direct impacts of temperature. Analysis approaches that represent surface flux as the summation of fluxes across a nonuniform soil profile may provide a means for handling transport-related lags and more accurately determining the temperature sensitivity of soil respiration.

Acknowledgements

Soil physical parameters were measured at the HJ Andrews Experimental Forest, which is funded by the National Science Foundation's Long-Term Ecological Research Program (DEB 08-23380), US Forest Service Pacific Northwest Research Station, and Oregon State University. Thanks to Carlos Sierra, Jonathan Martin, and three anonymous reviewers for helpful feedback.

References

Bahn M, Rodeghiero M, Anderson-Dunn M *et al*. (2008) Soil respiration in European grasslands in relation to climate and assimilate supply. *Ecosystems*, **11**, 1352–1367.

Bahn M, Schmitt M, Siegwolf R, Richter A, Brüggemann N (2009) Does photosynthesis affect grassland soil-respired CO_2 and its carbon isotope composition on a diurnal timescale? *New Phytologist*, **182**, 451–460.

Beltrami H (1996) Active layer distortion of annual air/soil thermal orbits. *Permafrost and Periglacial Processes*, **7**, 101–110.

Carbone MS, Vargas R (2008) Automated soil respiration measurements: new information, opportunities and challenges. *New Phytologist*, **177**, 295–297.

Carbone MS, Winston GC, Trumbore SE (2008) Soil respiration in perennial grass and shrub ecosystems: linking environmental controls with plant and microbial sources on seasonal and diel timescales. *Journal of Geophysical Research*, **113**, G02022, doi: 10.1029/2007JG000611.

Cerling T, Solomon DK, Quade J, Bowman JR (1991) On the isotopic composition of carbon in soil carbon dioxide. *Geochimica et Cosmochimica Acta*, **55**, 3403–3405.

Davidson EA, Janssens IA, Luo Y (2006a) On the variability of respiration in terrestrial ecosystems: moving beyond Q_{10}. *Global Change Biology*, **12**, 154–164.

Davidson EA, Savage KE, Trumbore SE, Borken W (2006b) Vertical partitioning of CO_2 production within a temperate forest soil. *Global Change Biology*, **12**, 944–956.

Ekblad A, Boström B, Holm A, Comstdet D (2005) Forest soil respiration rate and $\delta^{13}C$ is regulated by recent above ground weather conditions. *Oecologia*, **143**, 136–142.

Fessenden JE, Ehleringer JR (2003) Temporal variation in $\delta^{13}C$ of ecosystem respiration in the Pacific Northwest: links to moisture stress. *Oecologia*, **136**, 129–136.

Flechard CR, Neftel A, Jocher M, Ammann C, Leifeld J, Fuhrer J (2007) Temporal changes in soil pore space CO_2 concentration and storage under permanent grassland. *Agricultural and Forest Meteorology*, **142**, 66–84.

Gaumont-Guay D, Black A, Mccaughey H, Barr AG, Krishnan P, Jassal RS, Nesic Z (2008) Soil CO_2 efflux in contrasting boreal deciduous and coniferous stands and its contribution to the ecosystem carbon balance. *Global Change Biology*, **15**, 1302–1319.

Graf A, Weihermüller L, Huisman JA, Herbst M, Bauer J, Vereecken H (2008) Measurement depth effects on the apparent temperature sensitivity of soil respiration in field studies. *Biogeosciences*, **5**, 1175–1188.

Hillel D (1998) *Environmental Soil Physics*. Academic Press, San Diego.

Högberg P, Högberg MN, Göttlicher SG *et al*. (2008) High temporal resolution tracing of photosynthate carbon from the tree canopy to forest soil microorganisms. *New Phytologist*, **177**, 220–228.

Högberg P, Nordgern A, Buchmann N *et al*. (2001) Large-scale forest girdling shows that current photosynthesis drives soil respiration. *Nature*, **411**, 789–792.

Irvine J, Law BE, Anthoni P, Meinzer FC (2002) Water limtations to carbon exchange in old-growth and young Ponderosa pine stands. *Tree Physiology*, **22**, 189–196.

Irvine J, Law BE, Kurpius MR (2005) Coupling of canopy gas exchange with root and rhizosphere respiration in a semi-arid forest. *Biogeochemistry*, **73**, 271–282.

Jassal RS, Black TA, Cai T, Morgenstern K, Li Z, Gaumont-Guay D, Nesic Z (2007) Components of ecosystem respiration and an estimate of net primary productivity of an intermediate-aged Douglas-fir stand. *Agricultural and Forest Meteorology*, **144**, 44–57.

Kodoma N, Barnard RL, Salmon Y *et al*. (2008) Temporal dynamics of the carbon isotope composition in a *Pinus sylvestris* stand: from newly assimilated organic carbon to respired carbon dioxide. *Oecologia*, **156**, 737–750.

Kuzyakov Y, Gavrichkova O (2010) Time lag between photosynthesis and carbon dioxide efflux from soil: a review of mechanisms and controls. *Global Change Biology*. doi: 10.1111/j.1365-2486.2010.02179.x.

Liu Q, Edwards NT, Post WM, Gu L, Ledford J, Lenhart S (2006) Temperature-independent diel variation in soil respiration observed from a temperate deciduous forest. *Global Change Biology*, **12**, 2136–2145.

Mcdowell NG, Bowling DR, Bond BJ, Irvine J, Law BE, Anthoni P, Ehleringer JR (2004) Response of the carbon isotopic content of ecosystem, leaf, and soil respiration to meteorological and physiological driving factors in a *Pinus ponderosa* ecosystem. *Global Biogeochemical Cycles*, **18**, GB1013, doi: 10.1029/2003GB002049.

Mencuccini M, Höltta T (2010) The significance of phloem transport for the speed with which canopy photosynthesis and belowground respiration are linked. *New Phytologist*, **185**, 189–203.

Moldrup P, Olesen T, Schjonning P, Yamaguchi T, Rolston DE (2000) Predicting the gas diffusion coefficient in undisturbed soil from soil water characteristics. *Soil Science Society of America Journal*, **64**, 94–100.

Nickerson N, Risk D (2009) Physical controls on the isotopic composition of soil respired CO_2. *Journal of Geophysical Research*, **114**, G01013, doi: 10.1029/2008JG000766.

Ochsner TE, Horton R, Ren T (2001) A new perspective on soil thermal properties. *Soil Science Society of America Journal*, **65**, 1641–1647.

Pavelka M, Acosta M, Marek MV, Kutsch W, Janous D (2007) Dependence of the Q_{10} values on the depth on the the soil temperature measuring point. *Plant and Soil*, **292**, 171–179.

Pumpanen J, Ilvesniemi H, Hari P (2003) A process-based model for predicting soil carbon dioxide efflux and concentration. *Soil Science Society of America Journal*, **67**, 402–413.

Pypker T, Hauck M, Sulzman EW *et al*. (2008) Towards using $\delta^{13}C$ of ecosystem respiration to monitor canopy physiology in complex terrain. *Oecologia*, **158**, 399–410.

Reichstein M, Subke J-A, Angeli AC, Tenhunen JD (2005) Does the temperature sensitvity of decomposition of soil organic matter depend upon water content, soil horizon, or incubation time? *Global Change Biology*, **11**, 1754–1767.

Risk D, Kellman L, Beltrami H (2002) Carbon dioxide in soil profiles: production and temperature dependence. *Geophysical Research Letters*, **29**, 1087, doi: 10.1029/2001GL014002.

Risk D, Kellman L, Beltrami H, Diochon A (2008) *In situ* incubations highlight the environmental constraints on soil organic carbon decomposition. *Environmental Research Letters*, **3**, 04004, doi: 10.1088/1748-9326/3/4/044004.

Riveros-Iregui DA, Emanuel RE, Muth DJ *et al*. (2007) Diurnal hysteresis between soil CO_2 and soil temperature is controlled by soil water content. *Geophysical Research Letters*, **34**, L17404, doi: 10.1029/2007GL030938.

Ryan MG, Law BE (2005) Interpreting, measuring, and modeling soil respiration. *Biogeochemistry*, **73**, 3–27.

Stoy PC, Palmroth S, Oishi AC *et al*. (2007) Are ecosystem carbon inputs and outputs coupled at short time scales? A case study from adjacent pine and hardwood forests using impulse–response analysis. *Plant, Cell and Environment*, **30**, 700–710.

Tang J, Baldocchi DD, Xu L (2005) Tree photosynthesis modulates soil respiration on a diurnal time scale. *Global Change Biology*, **11**, 1298–1304.

Tedeschi V, Rey A, Manca G, Valentini R, Jarviss PG, Borghetti M (2006) Soil respiration in a Mediterranean oak forest at different developmental stages after coppicing. *Global Change Biology*, **12**, 110–121.

Trumbore SE (2006) Carbon respired by terrestrial ecosystems – recent progress and challenges. *Global Change Biology*, **12**, 141–153.

Vargas R, Allen MF (2008) Environmental controls and the influence of vegetation type, fine roots and rhizomorphs on diel and seasonal variation in soil respiration. *New Phytologist*, **179**, 460–471.

Supporting Information

Additional Supporting Information may be found in the online version of this article:

Appendix S1. The impacts of diel temperature range and Q_{10} on phase lags between surface flux and soil temperature.
Figure S1. Effect of A_0 on lag times between surface flux and temperature at the soil surface, and at 10 and 20cm depth.
Figure S2. Time series for surface flux at several Q_{10} values, in comparison to air and soil temperatures.

Please note: Wiley-Blackwell are not responsible for the content or functionality of any supporting materials supplied by the authors. Any queries (other than missing material) should be directed to the corresponding author for the article.